J. Fluid Mech. (2004), *vol.* 518, *pp.* 319–346.
DOI: 10.1017/S0022112004001120 Printed in the United Kingdom

A new asymptotic method for the analysis of convection in a rapidly rotating sphere

By KEKE ZHANG[1] AND XINHAO LIAO[2]

[1]Department of Mathematical Sciences, University of Exeter, EX4 4QE, UK
kzhang@ex.ac.uk

[2]Shanghai Astronomical Observatory, Chinese Academy of Sciences, China

(Received 24 March 2004 and in revised form 13 July 2004)

Thermal convection in rapidly rotating, self-gravitating Boussinesq fluid spheres is characterized by three parameters: the Rayleigh number R, the Prandtl number Pr and the Ekman number E. Two different asymptotic limits were considered in the previous studies of the linear problem. In the double limit $E \ll 1$ and $Pr/E \gg 1$, the local asymptotic theory showed that the convective motion is strongly non-axisymmetric, columnar, highly localized and described by the asymptotic scalings, $(1/s)\partial/\partial\phi = O\left(E^{-1/3}\right)$, $\partial/\partial z = O(1)$, $R_c = O\left(E^{-1/3}\right)$, where R_c denotes the critical Rayleigh number and (s, ϕ, z) are cylindrical polar coordinates with the axis of rotation at $s = 0$. A global asymptotic theory with novel features for the limit $E \ll 1$ and $Pr/E \gg 1$, indicating the radial asymptotic scaling $\partial/\partial s = O\left(E^{-1/3}\right)$, was recently developed by Jones *et al.* (*J. Fluid Mech.* vol. 405, 2000, p. 157). In the different double limit $E \ll 1$ and $Pr/E \ll 1$, an asymptotic theory for the onset of convection building upon the theory of inertial waves was developed by Zhang (*J. Fluid Mech.* vol. 268, 1994 p. 211). It was shown that the convective motion at the leading-order approximation is represented by a single inertial-wave mode with a quadratic polynomial of s and z, obeying the asymptotic dependence $\partial/\partial s \sim (1/s)\partial/\partial\phi = O(1)$, $\partial/\partial z = O(1)$ and $R_c = O(E)$ for stress-free spheres.

There exist no simple asymptotic scalings for $E \ll 1$ appropriate to all values of Pr/E. For an arbitrary small but non-zero E, the highly localized convection spreads out spatially with decreasing Pr, suggesting that the scaling laws such as $\partial/\partial s = O\left(E^{-1/3}\right)$ are no longer valid when Pr/E is not sufficiently large. This paper represents an attempt to develop a new asymptotic method for the analysis of convection in rapidly rotating spheres valid for asymptotically small E and for $0 \leqslant Pr/E < \infty$. The new method is based on the following three hypotheses. The first is that the leading-order velocity of convection for $0 \leqslant Pr/E < \infty$ at $E \ll 1$ is represented by either a single quasi-geostrophic-inertial-wave mode or by a combination of several quasi-geostrophic-inertial-wave modes convectively excited and sustained. Secondly, we assume that the convective motion for $0 \leqslant Pr/E < \infty$ at $E \ll 1$ always has columnar structure, i.e. $\partial/\partial z \sim O(1)$, but without the general asymptotic scalings in the radial and azimuthal direction. Thirdly, we assume that there always exists a boundary flow that is non-zero only in the Ekman boundary layer on the bounding spherical surface and plays an important role even in the case of stress-free boundaries. Comparison between the result of the new method and the corresponding fully numerical simulation demonstrates a satisfactory quantitative agreement for all values of $0 \leqslant Pr/E \leqslant O(10^6)$ when $O(10^{-5}) \leqslant E \leqslant O(10^{-6})$. The new method is asymptotic in the sense that it is valid only for an asymptotically small $E \ll 1$.

In addition to the linear problem of thermal convection in rapidly rotating spheres, the corresponding weakly nonlinear problem is also solved to obtain an analytical

expression for the convection-driven differential rotation generated by the nonlinear interaction of quasi-geostrophic-inertial-wave modes through the Reynolds stresses. The new method not only reveals the underlying nature of thermal convection in rapidly rotating spheres but also unites the two previously disjointed subjects in rotating fluids: the inertial-wave problem and the convective instability problem.

1. Introduction

First formulated and investigated by Chandrasekhar (1961), the problem of the onset of thermal convection in a rapidly rotating, self-gravitating Boussinesq fluid sphere driven by a uniform distribution of heat sources is classical and has been extensively studied (for example, Roberts 1968; Busse 1970, 1994; Soward 1977; Carrigan & Busse 1983; Fearn, Roberts & Soward 1988; Jones, Soward & Mussa 2000; Dormy *et al.* 2004). There are perhaps three major reasons why so much attention has been attracted to this classical problem: (i) it is of direct relevance to many geophysical and astrophysical bodies which are rotating rapidly and convecting, (ii) with only the two parameters involved, it represents the simplest mathematical problem for rotating spherical convection and (iii) it provides a fundamental understanding of the general physics and mechanisms for rotating spherical fluids. The current understanding of the problem can be found in an excellent review article by Busse (2002).

The convection problem in rotating spheres is characterized by three physical parameters: the Rayleigh number R, the Prandtl number Pr and the Ekman number E. The Rayleigh number R is effectively the ratio of destabilizing buoyancy forces to the Coriolis and dissipative forces, the Prandtl number Pr provides a measure of the relative importance of viscous and thermal diffusion and the Ekman number E is related to the ratio of viscous forces to the Coriolis force. In the problem of linear convective instability, the Rayleigh number R is completely determined by the Prandtl number Pr and the Ekman number E. Hence only the two parameters, E and Pr, are required to describe the properties of linear convection. For applications to many planetary fluid systems such as the Earth's liquid core, the Ekman number E is usually extremely small $E \ll 1$ and the Prandtl number Pr is moderately small $Pr = O(10^{-2})$ (for example, Gubbins & Roberts 1987). For a given small but non-zero E, the primary properties of the linear convection in a sphere such as the spatial and temporal structure of the flow are solely determined by the size of the Prandtl number Pr.

There were a number of important studies in the earlier research on linear convection in a rapidly rotating sphere after Chandrasekhar's formulation of the problem. Roberts (1968) and Busse (1970) established a local asymptotic theory for the onset of convection valid for the double limit $E \ll 1$ and $Pr/E \gg 1$. It was recognized that the linear convection is strongly non-axisymmetric and in the form of columnar rolls along the axis of rotation, highly localized in the neighbourhood of a critical cylinder whose radius is about half the radius of the sphere. The Roberts–Busse local theory assumed the following asymptotic scalings:

$$\frac{1}{s}\frac{\partial}{\partial \phi} = O\left(E^{-1/3}\right), \quad \frac{\partial}{\partial z} = O(1), \quad R_c = O\left(E^{-1/3}\right) \quad \text{for} \quad E \ll 1 \text{ and } Pr/E \gg 1, \quad (1)$$

where R_c denotes the critical Rayleigh number for the onset of convection and (s, ϕ, z) are cylindrical polar coordinates with $s = 0$ at the axis of rotation. The local

asymptotic theory requires only the boundary condition that the normal flow at the outer bounding spherical surface vanishes. Governed by a second-order ODE for z, the radial structure of the convection is undetermined by the local asymptotic theory. Soward (1977) was the first to point out that the exact critical Rayleigh number R_c for the onset of convection cannot be provided by the Roberts–Busse local asymptotic theory. He showed that disturbances at a Rayleigh number near the critical R_c predicted by the local asymptotic theory cannot be sustained and have to decay with time. The decay is caused by the fact that the radial frequency gradient, $\partial\omega/\partial s$, where ω is the frequency of linear convection, is non-zero, which results in phase mixing. When R is slightly different from R_c, the phase mixing leads to a shorter radial wavelength and the initial growing perturbation moves out of its unstable domain and hence decays with time (see also Soward & Jones 1983). It follows that the correct critical Rayleigh number for the onset of convection in the limit $E \ll 1$ and $Pr/E \gg 1$ must be associated with the vanishing radial frequency gradient.

An asymptotic theory for the onset of thermal convection in a rapidly rotating sphere for the different double limit $E \ll 1$ and $Pr/E \ll 1$ was developed by Zhang (1994) (see also Zhang & Busse 1987; Ardes, Busse & Wicht 1997). It was shown that the convective motion at leading order is represented by a single inertial wave mode that has the simple structure along the axis of rotation described by a quadratic polynomial of s and z. Buoyancy forces appear at next order to drive the inertial wave against the weak effects of viscous damping in the Ekman boundary layer. On the basis of the perturbation of the explicit inertial wave solution and taking into account the effects of the Ekman boundary layer, an explicit analytical solution for the onset of convection in the limit $E \ll 1$ and $Pr/E \ll 1$ was obtained. A quantitative agreement between the analytical and fully numerical analysis was also achieved, showing that the asymptotic scalings are given by

$$\frac{\partial}{\partial s} \sim \frac{1}{s}\frac{\partial}{\partial \phi} = O(1), \quad \frac{\partial}{\partial z} \leqslant O(1), \quad R_c = O(E) \quad \text{for} \quad E \ll 1 \text{ and } Pr/E \ll 1. \tag{2}$$

The asymptotic theory (Zhang 1994) for $Pr/E \ll 1$ and $E \ll 1$ was recently extended to the case of nearly thermally insulating boundary conditions by Busse & Simitev (2004) who also point out the importance of the azimuthal wavenumber $m = 1$.

There have been two important recent developments in rotating spherical convection. In the linear problem, a major breakthrough in the asymptotic theory for the onset of convection in the limit $E \ll 1$ and $Pr/E \gg 1$ was made by Jones *et al.* (2000). Suggested by the linear convection in the form of strongly radial spiralling (Zhang 1992), it was assumed that the radial scaling of the convection is given by $\partial/\partial s = O\left(E^{-1/3}\right)$. While the axial structure of the convection is governed by a second-order ODE which is the same as that in the Roberts–Busse local theory, the central issue in their asymptotic analysis is to extend the local solution onto the complex s-plan in which the phase mixing vanishes and then to determine the criterion for the onset of convection. Once the correct critical values of the Rayleigh number R_c, the wavenumber m_c and the frequency ω_c for the onset of convection are determined, the corresponding convection solution on the real axis is constructed such that the solution decays exponentially to zero on both sides of $s = s_M$, where s_M is the point at which the solution takes its maximum. They demonstrated that the fully numerical solutions are in good agreement with those obtained from the asymptotic analysis for $Pr \geqslant O(1)$ when $O(10^{-4}) \leqslant E \leqslant O(10^{-6})$. However, it should be pointed out that Pr has to be very much larger than E to be in this asymptotic regime, particularly, when $Pr \leqslant O(0.1)$. No satisfactory agreement between the asymptotic theory and full

numerics has been achieved for $Pr \leqslant O(0.1)$ even when $Pr/E = O(10^5)$. An extension of the Jones–Soward–Mussa asymptotic theory has been made to the case of linear convection in rapidly rotating spherical shells with a larger inner sphere for $Pr = 1$ (Dormy *et al.* 2004) and to the case of linear magnetoconvection in a rapidly rotating sphere in the presence of an imposed weak magnetic field (Jones, Mussa & Worland 2002).

In the nonlinear convection problem, motivated by explaining the observed strong zonal flow at the surfaces of Jupiter and Saturn, a number of numerical and laboratory experiments at large supercritical Rayleigh numbers have been carried out. Tilgner & Busse (1997, 1998) (see also Aurnou & Olson 2001; Christensen 2001, 2002) showed numerically that moderately nonlinear convection is dominated by the differential rotation (the mean zonal flow) when the spherical system has stress-free boundary conditions and the Ekman number E is sufficiently small, $E \leqslant O(10^{-4})$. It was also shown that the mean zonal flow is steady and quasi-geostrophic, nearly independent of the coordinate parallel to the axis of rotation for moderate supercritical Rayleigh numbers. An asymptotic nonlinear relation for large supercritical Rayleigh numbers was estimated numerically on the basis of systematic simulations over the wide range of the Rayleigh number (Christensen 2002). In laboratory experiments, strong zonal flows in rapidly rotating spherical systems were also observed (Sumita & Olson 2000; Aubert *et al.* 2001). Two important phenomena connected with a strong mean flow, localized convective motions and relaxation oscillations, were found in numerical simulations (Grote, Busse & Tilgner 2000; Grote & Busse 2001). In localized convection, the shearing action of a mean zonal flow inhibits thermal convection such that only in a certain region of longitude is convection strong enough to overcome the inhibiting effect. When the effect of the mean flow becomes too strong, the local intensification no longer suffices to offset the shearing effect on convection and the system chooses a temporal separation in the form of relaxation oscillations. The effect of a strong magnetic field on rotating spherical nonlinear convection was also studied (for example, Olson & Glatzmaier 1995; Sarson, Jones & Longbottom 1998).

This paper represents an attempt to develop a new asymptotic method for analysing the onset of thermal convection in a rapidly rotating, self-gravitating Boussinesq fluid sphere valid for $E \ll 1$ and $0 \leqslant Pr/E < \infty$. The new method follows the observation of the two known characteristics of convection in a rapidly rotating sphere. In the limits $E \ll 1$ and $Pr/E \gg 1$, the convection is on short length scales of $O(E^{1/3})$ and highly localized (Roberts 1968). However, in the limits $E \ll 1$ and $Pr/E \ll 1$, convection is on long length scales of $O(1)$ and described by a single inertial-wave mode (Zhang 1994). Evidently, the asymptotic scalings (1) must be violated when Pr/E decreases, indicating that there are no general asymptotic scalings such as (1) or (2) for $E \ll 1$ appropriate to all values of Pr/E. The new method builds on the three key hypotheses. The first hypothesis is that the leading-order solution of convective motion in a rapidly rotating sphere for $0 \leqslant Pr/E < \infty$ at $E \ll 1$ is represented by either a single quasi-geostrophic-inertial-wave (QGIW) mode or by a combination of several QGIW modes whose explicit analytical expression was determined by Zhang *et al.* (2001). It is worth mentioning that an explicit analytical expression for all inertial-wave modes in rotating spheroids of arbitrary eccentricity was also recently found (Zhang, Liao & Earnshaw 2004). Secondly, we assume that the convective motion for $0 \leqslant Pr/E < \infty$ at $E \ll 1$ always satisfies $\partial/\partial z \leqslant O(1)$, but without any particular asymptotic scalings in either the radial or azimuthal directions. Thirdly, we assume that there always exists an Ekman boundary layer flow on the bounding spherical surface even in the case of a stress-free boundary which is the focus of this paper.

It should be pointed out that the new method for the analysis of convection in rotating spheres is fundamentally different from the Galerkin spectral method which has been widely employed in the analysis of spherical convection (e.g. Zhang & Busse 1987; Ardes *et al.* 1997). In the Galerkin method, we expand an unknown variable, like the radial velocity, u_r, of a linear solution with an azimuthal wavenumber m, in terms of a certain set of functions satisfying all the required boundary conditions:

$$u_r(r,\theta,\phi,t)=\left[\sum_{k=1}^{K}\sum_{l=m}^{L}X_{lk}Y_l^m(\theta,\phi)\sin k\pi\frac{(r-r_i)}{(r_o-r_i)}\right]\mathrm{e}^{\mathrm{i}\omega t},\quad K\gg 1,\ L\gg m, \tag{3}$$

where (r,θ,ϕ) represent spherical polar coordinates, r_i and r_o denote the radii of the inner and outer spheres of a shell respectively, X_{lk} are coefficients to be determined, ω is the frequency of convection and $Y_l^m(\theta,\phi)$ with $l\geqslant m$ are spherical harmonics. There are three essential characteristics in the Galerkin expansion (3): (i) the expansion functions must be complete, (ii) the expansion must take the lowest-order members of a complete set of the functions and (iii) it can be used in either non-rotating or rotating convection in spherical systems. In contrast, the corresponding radial velocity in the new method is written as

$$u_r(r,\theta,\phi,t)=\left[\sum_{k}C_kU_{kr}(r,\theta,\phi)\right]\mathrm{e}^{\mathrm{i}\omega t}\quad\text{for}\quad E\ll 1, \tag{4}$$

where C_k are coefficients and U_{kr} is the radial velocity of a QGIW mode with an azimuthal wavenumber m (see §§4.1 and 4.2 for details). There are three important features in (4): (i) the expansion functions in terms of QGIW modes are incomplete and do not satisfy all the required boundary conditions; (ii) dependent upon the value of Pr, the expansion (4) takes either one term or a small number of terms which are usually not associated with the lowest-order members of QGIW modes, and (iii) the expansion (4) can be only used for convection in rapidly rotating spheres with an asymptotically small E. In other words, the expansion (4) reflects or postulates the underlying physical nature of thermal convection in a rapidly rotating sphere: the leading-order convection solution for an asymptotically small $E\ll 1$ is formed from either a single or a small number of QGIW modes.

In this paper, we undertake an analysis based on the new asymptotic method as well as the corresponding fully numerical simulations in a rapidly rotating spherical shell with a small inner sphere for a wide range of the Prandtl number $0\leqslant Pr\leqslant O(1)$. A satisfactory quantitative agreement between the new method and fully numerical simulations is achieved for all cases studied in the asymptotic regime $O(10^{-5})\leqslant E\leqslant O(10^{-6})$.

This paper also represents an attempt to derive the first explicit analytical expression for the convection-driven differential rotation near the onset of thermal convection in the whole fluid sphere. After solving the linear problem of convective instability, the corresponding weakly nonlinear problem is solved to obtain an analytical expression for the differential rotation generated by the nonlinear interaction of QGIW modes through the Reynolds stresses. We show analytically that the mean zonal flow is quasi-geostrophic, steady and predominant if E is sufficiently small, consistent with the results of the existing nonlinear numerical simulations.

The remainder of the paper is organized as follows. After discussing the mathematical formulation of thermal convection in §2, we briefly outline the previous asymptotic theories in §3 and the results of our new asymptotic method and analysis

are presented in § 4. Section 5 closes the paper with a brief summary and some remarks.

2. Mathematical formulation of the problem

We consider a Boussinesq fluid sphere of radius r_o with constant thermal diffusivity κ, thermal expansion coefficient α and kinematic viscosity ν. The fluid sphere rotates uniformly with a constant angular velocity $\boldsymbol{\Omega}$ in the presence of its own gravitational field

$$\boldsymbol{g} = -\gamma \boldsymbol{r}, \tag{5}$$

where γ is a positive constant and $\boldsymbol{r}$ is the position vector with its origin at the centre of the sphere. A traditional heating model (Chandrasekhar 1961; see also Roberts 1968; Busse 1970; Jones *et al.* 2000) is adopted, in which the basic unstable conducting temperature gradient,

$$\nabla T_s = -\beta \boldsymbol{r}, \tag{6}$$

where β is a positive constant, is produced by a uniform distribution of heat sources in the whole sphere. The problem of thermal convection, which was first formulated by Chandrasekhar (1961), is governed by the following three equations:

$$\frac{\partial \boldsymbol{u}}{\partial t} + \boldsymbol{u}\cdot\nabla\boldsymbol{u} + 2\boldsymbol{\Omega}\times\boldsymbol{u} = -\frac{1}{\rho}\nabla p + \gamma\alpha\Theta\boldsymbol{r} + \nu\nabla^2\boldsymbol{u}, \tag{7}$$

$$\frac{\partial \Theta}{\partial t} + \boldsymbol{u}\cdot\nabla\Theta = \beta\boldsymbol{u}\cdot\boldsymbol{r} + \kappa\nabla^2\Theta, \tag{8}$$

$$\nabla\cdot\boldsymbol{u} = 0. \tag{9}$$

where t is time, ρ is the fluid density, Θ represents the deviation of the temperature from its static distribution $T_s(r)$, p is the total pressure and $\boldsymbol{u}$ is the three-dimensional velocity field: $\boldsymbol{u} = (u_s, u_\phi, u_z)$ in cylindrical polar coordinates (s, ϕ, z) or $\boldsymbol{u} = (u_r, u_\theta, u_\phi)$ in spherical polar coordinates (r, θ, ϕ). We have absorbed the centrifugal force, $\rho\boldsymbol{\Omega}\times(\boldsymbol{\Omega}\times\boldsymbol{r})$, into the pressure p since it is usually much smaller than the Coriolis force $2\boldsymbol{\Omega}\times\boldsymbol{u}$ (Chandrasekhar 1961). In (7), the term $\alpha\gamma\Theta\boldsymbol{r}$ represents the buoyancy force that drives thermal convection and provides a coupling to the heat equation (8).

We shall employ the radius of the sphere r_o as the length scale, $1/\Omega$ as the unit of time and $\beta r_o^2\nu/\kappa$ as the unit of temperature fluctuation of the system, which leads to the dimensionless equations

$$\frac{\partial \boldsymbol{u}}{\partial t} + \boldsymbol{u}\cdot\nabla\boldsymbol{u} + 2\boldsymbol{k}\times\boldsymbol{u} = -\nabla p + 2E(R\Theta\boldsymbol{r} + \nabla^2\boldsymbol{u}), \tag{10}$$

$$Pr\frac{\partial \Theta}{\partial t} + \boldsymbol{u}\cdot\nabla\Theta = \boldsymbol{u}\cdot\boldsymbol{r} + 2E\nabla^2\Theta, \tag{11}$$

$$\nabla\cdot\boldsymbol{u} = 0, \tag{12}$$

where $\boldsymbol{k}$ is a unit vector parallel to the axis of rotation. The three non-dimensional parameters, the Rayleigh number R, the Prandtl number Pr and the Ekman number E, are defined as

$$R = \frac{\alpha\beta\gamma r_o^4}{\Omega\kappa}, \qquad Pr = \frac{\nu}{\kappa}, \qquad E = \frac{\nu}{2\Omega r_o^2}.$$

Note that the relationship between the definition of the Rayleigh number given by Chandrasekhar (1961) R_{ch} and our Rayleigh number R is $R = 2ER_{ch}$. All the variables in the rest of the paper will be non-dimensional.

A weakly nonlinear solution near the onset of convection is expanded as

$$\left.\begin{aligned} \boldsymbol{u} &= \epsilon(\boldsymbol{u}_0 + \boldsymbol{u}_0^*) + \frac{\epsilon^2}{2E} U(r\sin\theta)\hat{\boldsymbol{\phi}} + \cdots, \\ p &= 2\epsilon(p_0 + p_0^*) + \epsilon^2(p_1 + p_1^*)\cdots, \\ \Theta &= \epsilon(\Theta_0 + \Theta_0^*) + \cdots, \\ R &= R_0 + \cdots, \end{aligned}\right\} \tag{13}$$

where ϵ is the amplitude of linear convection, U is the differential rotation generated by the nonlinear interaction of QGIW modes and Z^* denotes the complex conjugate of Z. A linear solution of convection is then expressed in the form of an azimuthally travelling wave

$$[\boldsymbol{u}_0, p_0, \Theta_0](r, \theta, \phi, t) = [\boldsymbol{u}_0, p_0, \Theta_0](r, \theta, \phi)\exp(2\mathrm{i}\sigma t), \tag{14}$$

where σ is the half-frequency of convection. The leading-order problem for the onset of convection is governed by

$$\mathrm{i}\sigma\boldsymbol{u}_0 + \boldsymbol{k}\times\boldsymbol{u}_0 = -\nabla p_0 + E(R_0\Theta_0\boldsymbol{r} + \nabla^2\boldsymbol{u}_0), \tag{15}$$

$$\mathrm{i}Pr\sigma\Theta_0 = \tfrac{1}{2}\boldsymbol{u}_0\cdot\boldsymbol{r} + E\nabla^2\Theta_0, \tag{16}$$

$$\nabla\cdot\boldsymbol{u}_0 = 0. \tag{17}$$

The velocity boundary conditions assumed in this paper are stress-free and impenetrable, which give

$$\frac{\partial(\hat{\boldsymbol{\phi}}\cdot\boldsymbol{u}_0/r)}{\partial r} = \frac{\partial(\hat{\boldsymbol{\theta}}\cdot\boldsymbol{u}_0/r)}{\partial r} = \hat{\boldsymbol{r}}\cdot\boldsymbol{u} = 0 \tag{18}$$

at the outer bounding spherical surface $r = 1$. Perfect thermally conducting boundaries impose the condition

$$\Theta_0 = 0 \quad \text{at} \quad r = 1. \tag{19}$$

Linear solutions of the convection problem defined by (15)–(17) subject to the boundary conditions (18)–(19) will be sought and discussed in § 4.

For the purpose of comparison, we also undertake fully numerical simulations for the linear problem in rotating spherical shells. In the numerical simulations, we expand the velocity $\boldsymbol{u}_0$ as a sum of poloidal (v_0) and toroidal vectors (w_0):

$$\boldsymbol{u}_0 = \nabla\times\nabla\times\boldsymbol{r}v_0 + \nabla\times\boldsymbol{r}w_0. \tag{20}$$

Making use of the above expression and applying $\boldsymbol{r}\cdot\nabla\times$ and $\boldsymbol{r}\cdot\nabla\times\nabla\times$ to (15), we derive the three independent non-dimensional scalar equations,

$$\left[E\nabla^2 + (1-\eta)^2\left(\frac{\partial}{\partial\phi} - \mathrm{i}\sigma\mathscr{L}\right)\right]\nabla^2 v_0 + (1-\eta)^2\,\mathscr{Q}w_0 - (1-\eta)^4\,ER_0\mathscr{L}\Theta_0 = 0, \tag{21}$$

$$\left[E\nabla^2 + (1-\eta)^2\left(\frac{\partial}{\partial\phi} - \mathrm{i}\sigma\mathscr{L}\right)\right]w_0 - (1-\eta)^2\,\mathscr{Q}v_0 = 0, \tag{22}$$

$$[E\nabla^2 - \mathrm{i}(1-\eta)^2\sigma Pr]\Theta_0 + \tfrac{1}{2}(1-\eta)^2\,\mathscr{L}v_0 = 0, \tag{23}$$

where η is the ratio of the inner sphere radius (r_i) to the outer sphere radius (r_o), $\eta = r_i/r_o$, and the differential operators, $\mathscr{L}$ and $\mathscr{Q}$, are defined as

$$\mathscr{L} = -r^2\nabla^2 + \frac{\partial}{\partial r}r^2\frac{\partial}{\partial r}, \quad \mathscr{Q} = \boldsymbol{k}\cdot\nabla - \tfrac{1}{2}(\mathscr{L}\boldsymbol{k}\cdot\nabla + \boldsymbol{k}\cdot\nabla\mathscr{L}).$$

For full numerics in a rotating spherical shell, the inner sphere is set to be sufficiently small at $\eta = 0.01$ that a solution in the spherical shell can be directly compared to that obtained in a sphere. Note that the factor $(1-\eta)$ comes from the different length scale, which is the thickness of the spherical shell, used in our numerical simulations.

The assumptions of impenetrable, perfectly thermally conducting and stress free boundaries impose the following boundary conditions at the inner and outer bounding spherical surfaces

$$v_0 = \Theta_0 = \frac{\partial^2 v_0}{\partial r^2} = \frac{\partial}{\partial r}\left(\frac{w_0}{r}\right) = 0 \quad \text{at} \quad r_i = \frac{\eta}{(1-\eta)}, \quad r_o = \frac{1}{(1-\eta)}. \tag{24}$$

We shall not discuss the details of the numerical method for solving the linear problem which was discussed in Zhang (1992) (see also Zhang & Busse 1987).

In this paper, the results such as the critical Rayleigh number R_c (the smallest R_0) for the onset of convection obtained from the full numerics are denoted by a subscript *FNUM* while the results derived from the new method are denoted by a subscript *QGIW*.

3. Previous theories for $E \ll 1$ and $Pr/E \gg 1$

To appreciate the distinct features of the new analysis in this paper, it is helpful to take a brief look at the previous asymptotic theories for the onset of thermal convection in a rapidly rotating sphere ($E \ll 1$) valid for $Pr/E \gg 1$.

3.1. *Roberts–Busse asymptotic theory*

In the Robert–Busse local asymptotic analysis (Roberts 1968; Busse 1970), the velocity $\boldsymbol{u}_0$ is expressed as a sum of poloidal and toroidal vectors

$$\boldsymbol{u}_0 = \nabla\times(\boldsymbol{k}\Psi) + \boldsymbol{k}W, \tag{25}$$

with Ψ and W being written in the form

$$(W, \Psi) = [W(z), \Psi(z)]\exp[\mathrm{i}(ks + m\phi + \omega t)], \tag{26}$$

where k is the radial wavenumber and m is the azimuthal wavenumber. In other words, both the radial and azimuthal dependences are assumed to be sinusoidal. Making use of (25) and applying $\boldsymbol{k}\cdot\nabla\times$ and $\boldsymbol{k}\cdot\nabla\times\nabla\times$ to the momentum equation, they derived a system of ODEs:

$$\frac{\mathrm{d}W}{\mathrm{d}z} = \left[E\left(k^2 + \frac{m^2}{s^2}\right) + \mathrm{i}\frac{\omega}{2}\right]\left(k^2 + \frac{m^2}{s^2}\right)\Psi + \mathrm{i}mR_0\Theta_0, \tag{27}$$

$$\frac{\mathrm{d}\Psi}{\mathrm{d}z} = \left[E\left(k^2 + \frac{m^2}{s^2}\right) + \mathrm{i}\frac{\omega}{2}\right]W - zER_0\Theta_0, \tag{28}$$

$$zW = \left[2E\left(k^2 + \frac{m^2}{s^2}\right) + \mathrm{i}Pr\omega\right]\Theta_0 - \mathrm{i}m\Psi. \tag{29}$$

The above three equations can be combined into a single second-order ODE for $W(z)$:

$$\frac{\mathrm{d}^2 W}{\mathrm{d}z^2} = \mathscr{F}(\hat{\omega}, \hat{R}_0, Pr, s, z, \hat{k}^2, \hat{m}) W(z) = 0, \tag{30}$$

where $\hat{\omega}, \hat{R}_0, \hat{k}^2, \hat{m}$ are scaled in accordance with the assumed asymptotic dependence (1) on which the asymptotic local theory hinges. The second-order ODE (30) is solved subject to the normal flow boundary condition $\boldsymbol{u}_0 \cdot \hat{\boldsymbol{r}} = 0$ at $r = 1$:

$$\frac{\mathrm{d}W}{\mathrm{d}z} + \mathscr{G}(\hat{\omega}, s, \hat{k}^2, \hat{m}) z W(z) = 0 \quad \text{at} \quad z = \sqrt{1 - s^2} \tag{31}$$

and

$$W = 0 \quad \text{at} \quad z = 0. \tag{32}$$

It should be noted that the system (27)–(29) possesses an equatorial symmetry that allows separation of the solution into two distinct families. The condition (32) selects the following equatorial symmetry:

$$(u_{0s}, u_{0z}, u_{0\phi})(s, z, \phi) = (u_{0s}, -u_{0z}, u_{0\phi})(s, -z, \phi), \tag{33}$$

which corresponds to the most unstable convection mode (Busse 1970). The other family with the opposite equatorial symmetry,

$$(u_{0s}, u_{0z}, u_{0\phi})(s, z, \phi) = (-u_{0s}, u_{0z}, -u_{0\phi})(s, -z, \phi), \tag{34}$$

will be not considered in this paper.

Since there is no $\partial/\partial s$ involved in either the governing equation (30) or in the boundary condition (31), (30) has to be solved for a given value of s (the characteristics of a local asymptotic theory). At the onset of convection, the perturbation is neither decaying nor growing, which requires

$$\mathrm{Im}[\hat{\omega}] = 0. \tag{35}$$

The minimization of the Rayleigh number over the scaled radial wavenumber $\hat{k}$, the scaled azimuthal wavenumber $\hat{m}$ and the location of the convection s gives

$$\mathrm{Im}\left[\frac{\partial \hat{\omega}}{\partial \hat{k}}\right] = 0, \qquad \mathrm{Im}\left[\frac{\partial \hat{\omega}}{\partial \hat{m}}\right] = 0, \qquad \mathrm{Im}\left[\frac{\partial \hat{\omega}}{\partial s}\right] = 0. \tag{36}$$

For given values of $\hat{k}, \hat{m}$ and s, the second-order ODE (30) satisfying the boundary conditions (31) and (32) can be readily solved numerically. The numerical solution for the ODE is then used to compute the relevant partial derivatives via an appropriate scheme of finite differences. An iterative procedure is then employed to solve the four equations given by (35)–(36) numerically. For example, Busse (1970) found that at the onset of convection

$$s_c = 0.5004, \quad m_c = 0.3003 E^{-1/3}, \quad R_c = 3.382 E^{-1/3} \quad \text{for} \quad Pr = 1.0. \tag{37}$$

The dependence of ω on k is always through k^2. By implication, the first equation in (36) gives $k_c = 0$ at $R_0 = R_c$. Consequently, the radial structure of the convection and the precise asymptotic scaling in the radial direction cannot be determined by the local asymptotic analysis. Furthermore, there is phase mixing, $\mathrm{Re}(\partial\omega/\partial s) \neq 0$, which leads to the decay of any initial disturbance near the onset of convection, a critically important character of the local asymptotic theory first pointed out by Soward (1977).

3.2. *Jones–Soward–Mussa asymptotic theory*

In order to remove the phase mixing, Jones *et al.* (2000) considered the analytic extension of the entire problem (all variables and parameters) defined by (30)–(32) onto the complex s-plane. At the onset of convection, they require that both the complex group velocity and complex phase mixing are zero at $s = s_c$. Hence the conditions (35)–(36) in the Roberts–Busse asymptotic theory are replaced by

$$\mathrm{Im}[\hat{\omega}] = 0, \tag{38}$$

$$\left[\frac{\partial \hat{\omega}}{\partial \hat{k}}\right]_{complex} = 0, \tag{39}$$

$$\left[\frac{\partial \hat{\omega}}{\partial \hat{m}}\right]_{complex} = 0, \qquad \left[\frac{\partial \hat{\omega}}{\partial s}\right]_{complex} = 0, \tag{40}$$

together with the requirements that

$$\mathrm{Im}[\hat{R}_0] = 0, \qquad \mathrm{Im}[\hat{m}] = 0. \tag{41}$$

While the condition given by (39) gives rise to the complex $\hat{k} = 0$, one real unknown $\hat{\omega}$ and the six unknowns in the three complex unknowns ($\hat{m}$, $\hat{R}_0$, s) are determined by solving the seven real equations (one given by (38), four in (40), two in (41)) through a numerical iteration procedure employing a finite difference scheme. For example, they found at the onset of convection

$$s_c = 0.5342 - \mathrm{i}0.0967, \quad m_c = 0.3029E^{-1/3}, \quad R_c = 4.117E^{-1/3} \quad \text{for} \quad Pr = 1.0. \tag{42}$$

Once the values of $\hat{\omega}_c$, $\hat{m}_c$ and $\hat{R}_c$ are determined, the corresponding solution on the real axis can be constructed such that $\mathrm{Im}(\hat{k}) = 0$ on the real s-axis. It was shown that

$$\frac{\partial}{\partial s} \sim \frac{1}{s}\frac{\partial}{\partial \phi} = O\left(E^{-1/3}\right), \quad \frac{\partial}{\partial z} = O(1), \quad R_c = O\left(E^{-1/3}\right) \quad \text{for} \quad E \ll 1 \text{ and } Pr/E \gg 1. \tag{43}$$

They found that the agreement between the asymptotic analysis and full numerics is satisfactory for $Pr \geqslant O(1)$. However, the agreement is poor for $Pr \leqslant O(0.1)$ even at a very small Ekman number $E = O(10^{-6})$.

In fact, a satisfactory agreement between the asymptotic analysis and full numerics has not been achieved for moderate Prandtl numbers $Pr \leqslant O(0.1)$ in all the previous asymptotic theories. We believe that the poor agreement for $Pr \leqslant O(0.1)$ reflects the fact that the convective flow spreads out quickly with diminishing Pr. When the convection becomes less localized, the assumptions leading to the ODEs (27)–(29) or (30) are no long valid and in the present analysis we must solve the corresponding system of PDEs discussed below.

4. A new asymptotic method for $E \ll 1$ with $0 \leqslant Pr/E < \infty$

4.1. *Hypotheses*

The new asymptotic method for the analysis of thermal convection in a rapidly rotating sphere for $0 \leqslant Pr/E < \infty$ at $E \ll 1$ is based on the following three hypotheses.

The first hypothesis: For an arbitrary small but non-zero $E \ll 1$, the asymptotic analysis for $Pr/E \gg 1$ (Roberts 1968; Busse 1970; Jones *et al.* 2000) suggests that $\partial/\partial s \sim \partial/s\partial\phi = O\left(E^{-1/3}\right)$ while the asymptotic analysis for $Pr/E \ll 1$ (Zhang 1994)

indicates $\partial/\partial s \sim \partial/s\partial\phi = O(1)$. It follows that, for the general case $0 \leqslant Pr/E < \infty$ at $E \ll 1$, we have to assume

$$O(1) \leqslant \frac{\partial}{\partial s} \leqslant O\left(E^{-1/3}\right), \qquad O(1) \leqslant \frac{1}{s}\frac{\partial}{\partial \phi} \leqslant O\left(E^{-1/3}\right). \tag{44}$$

In other words, we hypothesize that there exists no simple asymptotic scalings at $E \ll 1$, such as that given by (1) or (2), valid for $0 \leqslant Pr/E < \infty$. However, we shall always assume that the flow has columnar structure (quasi-geostrophic)

$$\frac{\partial}{\partial z} \leqslant O(1). \tag{45}$$

A consequence of this hypothesis is that we must solve PDEs for convection given by (15–17).

The second hypothesis: For an arbitrary small but non-zero $E \ll 1$, the asymptotic analysis for $Pr/E \gg 1$ (Roberts 1968; Busse 1970; Jones *et al.* 2000) suggest that the Ekman boundary layer (hence the type of the velocity boundary condition) does not play a leading role. However, the asymptotic analysis for $Pr/E \ll 1$ (Zhang 1994) indicates that the Ekman boundary layer, even in the case of stress-free boundaries, plays an essential role. For the general case $0 \leqslant Pr/E < \infty$ at $E \ll 1$, we hypothesize that there always exists a boundary flow, $\tilde{\boldsymbol{u}}_0$, that is non-zero only in the Ekman boundary layer on the bounding spherical surface such that

$$\hat{\boldsymbol{r}} \cdot \nabla \left[\frac{\boldsymbol{r}}{r^2} \times (\boldsymbol{u}_0 + \tilde{\boldsymbol{u}}_0)\right] = 0, \tag{46}$$

even though the effect of the Ekman boundary layer on convection may be of secondary importance in the case of stress-free boundaries with $Pr \geqslant O(1)$.

The third hypothesis: For an arbitrary small but non-zero $E \ll 1$, the leading-order velocity of convection $\boldsymbol{u}_0$ at $Pr/E \to 0$ is given by a single QGIW mode

$$\boldsymbol{u}_0 = (\boldsymbol{U}_1 + \tilde{\boldsymbol{U}}_1)\mathrm{e}^{2\mathrm{i}\sigma t}, \tag{47}$$

where $\boldsymbol{U}_1(s, z, \phi)$ is a quadratic polynomial of s and z with m-periodicity ($m \geqslant 1$) in the azimuthal direction, $\tilde{\boldsymbol{U}}_1$ is the Ekman-boundary-layer flow and $\boldsymbol{U}_1$ satisfies

$$\mathrm{i}\sigma_1 \boldsymbol{U}_1 + \hat{\boldsymbol{z}} \times \boldsymbol{U}_1 = -\nabla P_1, \tag{48}$$

$$\nabla \cdot \boldsymbol{U}_1 = 0, \tag{49}$$

subject to

$$\hat{\boldsymbol{r}} \cdot \boldsymbol{U}_1 = 0, \tag{50}$$

where σ_1 is the half-frequency of the QGIW mode. When Pr/E increases, we anticipate that more than one QGIW modes with the higher degree of polynomials are convectively excited and coupled together. This leads to the hypothesis that the leading-order velocity of thermal convection for $0 \leqslant Pr/E < \infty$ is expressed in the form

$$\boldsymbol{u}_0 = \sum_N [C_N(\boldsymbol{U}_N + \tilde{\boldsymbol{U}}_N)]\mathrm{e}^{2\mathrm{i}\sigma t}, \tag{51}$$

where C_N are complex coefficients and $\boldsymbol{U}_N(s, z, \phi)$ represents a QGIW mode satisfying

$$\mathrm{i}\sigma_N \boldsymbol{U}_N + \hat{\boldsymbol{z}} \times \boldsymbol{U}_N = -\nabla P_N, \tag{52}$$

$$\nabla \cdot \boldsymbol{U}_N = 0, \tag{53}$$

which are subject to

$$|\sigma_N| \ll 1, \ \hat{\boldsymbol{r}} \cdot \boldsymbol{U}_N = 0 \quad \text{at} \quad r = 1, \tag{54}$$

where $\boldsymbol{U}_N$ is a polynomial of s and z of degree $2N$ with m-periodicity ($m \geqslant 1$) in the azimuthal direction and σ_N is the half-frequency of a QGIW mode $\boldsymbol{U}_N$. In the expansion (51), we introduce the Ekman-layer flow $\tilde{\boldsymbol{U}}_N$ for a stress-free boundary such that $(\boldsymbol{U}_N + \tilde{\boldsymbol{U}}_N)$ satisfies

$$\hat{\boldsymbol{r}} \cdot \nabla \left[\frac{\boldsymbol{r}}{r^2} \times (\boldsymbol{U}_N + \tilde{\boldsymbol{U}}_N) \right] = 0. \tag{55}$$

Our analysis is asymptotic in the sense that it is valid only for an asymptotically small Ekman number $E \ll 1$. In comparison with the previous asymptotic analysis, there is no restriction on the size of Pr/E in the present analysis.

It is worth mentioning that the unanswered mathematical question regarding the completeness of the inviscid inertial modes, raised by Greenspan (1968), is irrelevant to the new method. Our assumption is only concerned with the underlying nature of thermal convection in a rapidly rotating sphere: the leading-order convective flow consists of either a single or a small number of QGIW modes with low frequencies $|\sigma_N| \ll 1$.

4.2. *QGIW (quasi-geostrophic-inertial-wave) modes*

A general explicit expression for QGIW modes in a rotating sphere was recently found by Zhang *et al.* (2001)(see also Liao, Zhang & Earnshaw 2001). For the analysis of the convection problem, it is mathematically convenient to express the QGIW modes (i.e. solutions of (52)–(53) satisfying the boundary condition (54)) using spherical polar coordinates

$$\boldsymbol{U}_N = [\hat{\boldsymbol{r}} \cdot \boldsymbol{U}_N, \hat{\boldsymbol{\phi}} \cdot \boldsymbol{U}_N, \hat{\boldsymbol{\theta}} \cdot \boldsymbol{U}_N] = \frac{1}{Q_N} [\mathrm{i} U_{Nr}, U_{N\phi}, \mathrm{i} U_{N\theta}] \mathrm{e}^{\mathrm{i}m\phi}, \tag{56}$$

where the three real functions $(U_{Nr}, U_{N\phi}, U_{N\theta})$ are given by

$$\begin{aligned} U_{N\theta} = &- \sum_{i=0}^{N} \sum_{j=0}^{N-i} r^{m+2(i+j)-1} C_{ijmN} \sigma_N^{2i-1} \left(1 - \sigma_N^2\right)^{j-1} \sin^{m+2j-1}\theta \cos^{2i-1}\theta \\ &\times \left[\sigma_N (m + m\sigma_N + 2j\sigma_N) \cos^2\theta + 2i \left(1 - \sigma_N^2\right) \sin^2\theta\right], \end{aligned} \tag{57}$$

$$U_{N\phi} = \sum_{i=0}^{N} \sum_{j=0}^{N-i} r^{m+2(i+j)-1} C_{ijmN} \sin^{m+2j-1}\theta \cos^{2i}\theta \sigma_N^{2i} \left(1 - \sigma_N^2\right)^{j-1} (m + m\sigma_N + 2j), \tag{58}$$

$$\begin{aligned} U_{Nr} = &- \sum_{i=0}^{N} \sum_{j=0}^{N-i} r^{m+2(i+j)-1} C_{ijmN} \sigma_N^{2i-1} \left(1 - \sigma_N^2\right)^{j-1} \sin^{m+2j}\theta \cos^{2i}\theta \\ &\times \left[\sigma_N (m + m\sigma_N + 2j\sigma_N) - 2\mathrm{i}\left(1 - \sigma_N^2\right)\right]. \end{aligned} \tag{59}$$

In (57)–(59), N is a positive integer and C_{ijmN} is defined as

$$C_{ijmN} = \frac{(-1)^{i+j} [2(N + i + j + m) - 1]!!}{2^{j+1} (2i - 1)!! (N - i - j)! i! j! (m + j)!},$$

N	σ_N
1	−0.12826577307
2	−0.07250885363
3	−0.04840665659
4	−0.03511732822
5	−0.02683168605
6	−0.02125438088
7	−0.01729489865
8	−0.01437061081
9	−0.01214348353
10	−0.01040492969

TABLE 1. Examples of half-frequencies σ_N for quasi-geostrophic-inertial-wave (QGIW) modes obtained from (62) at $m=8$ for different values of N.

where $n!$ and $(2n-1)!!$ are defined as

$$n!=n(n-1)\cdots(2)(1),\ \ (2n-1)!!=(2n-1)(2n-3)\cdots(3)(1).$$

All the QGIW modes have equatorial symmetry (33) and the normalization factor Q_N is given by

$$Q_N^2=\sum_{i=0}^{N}\sum_{j=0}^{N-i}\sum_{k=0}^{N}\sum_{l=0}^{N-k}\pi 2^{j+l+m-1}C_{ijmN}C_{klmN}\sigma_N^{2(i+k-1)}\left(1-\sigma_N^2\right)^{j+l}$$
$$\times\frac{(m+j+l-1)!(2i+2k-3)!!}{[2(m+j+l+i+k)+1)!!}\left\{\frac{\sigma_N^2 S_{jl}[2(i+k)-1]}{1-\sigma_N^2}+8ik(m+j+l)\right\},\quad(60)$$

where

$$S_{jl}=(2j\sigma_N+m\sigma_N+m)(2l\sigma_N+m\sigma_N+m)+(2j+m\sigma_N+m)(2l+m\sigma_N+m).$$

We choose

$$\int_V \boldsymbol{U}_N\cdot\boldsymbol{U}_M^*\,\mathrm{d}V=\delta_{NM}.\quad(61)$$

Except for the special case $Pr/E\to 0$, we are interested in the QGIW modes characterized by $|\sigma_N|\ll 1$. For a non-zero azimuthal wavenumber m, there are $2N$ different inertial-wave modes whose half-frequencies σ_N satisfy

$$0=m+\sum_{j=0}^{N-1}(-1)^{j+N}\left\{\frac{N![2(2N+m-j)]!(N+m)!}{[2(N-j)]![2(N+m)]!j!(2N+m-j)!}\right\}$$
$$\times[m\sigma_N-2(1-\sigma_N)(N-j)]\sigma_N^{2N-2j-1},\quad(62)$$

which results from the normal flow condition $U_{Nr}=0$ at $r=1$ given by (59). Among $2N$ different inertial-wave modes for a given N and m, QGIW modes correspond to the inertial-wave modes that are travelling slowly in the azimuthal direction with $|\sigma_N|\ll 1$. Several examples of σ_N for the QGIW modes obtained from (62) at $m=8$ with different values of N are given in table 1.

4.3. *Formulation*

Substituting (51) into the momentum equation, multiplying the resulting equation by $\boldsymbol{U}_M^*$, the complex conjugate of $\boldsymbol{U}_M$, and integrating the equation over the sphere, we

obtain

$$C_M \mathrm{i}(\sigma - \sigma_M) = E\left(R_0 \int_V \boldsymbol{U}_M^* \cdot \boldsymbol{r}\Theta \,\mathrm{d}V + 2\sum_N C_N \int_S \boldsymbol{U}_M^* \cdot \boldsymbol{U}_N \,\mathrm{d}S\right) - E\left(\sum_N C_N \int_V \nabla \times \boldsymbol{U}_M^* \cdot \nabla \times \boldsymbol{U}_N \,\mathrm{d}V\right), \quad M = 1, 2, 3, \ldots, \tag{63}$$

where σ_M is the half-frequency of a QGIW mode $\boldsymbol{U}_M$, $\int_V \mathrm{d}V$ represents the volume integral over the sphere and $\int_S \mathrm{d}S$ represents the surface integral over the outer spherical surface at $r = 1$. In deriving (63), we have used the properties

$$\left.\begin{aligned} &\int_V \boldsymbol{U}_M^* \cdot \nabla P_N \,\mathrm{d}V = 0, \\ &\int_V \boldsymbol{U}_M^* \cdot (\boldsymbol{k} \times \boldsymbol{U}_N) \,\mathrm{d}V = -\mathrm{i}\sigma_M \delta_{MN}, \\ &\int_V \boldsymbol{U}_M^* \cdot \nabla^2 (\boldsymbol{U}_N + \tilde{\boldsymbol{U}}_N) \,\mathrm{d}V = 2\int_S \boldsymbol{U}_M^* \cdot \boldsymbol{U}_N \,\mathrm{d}S - \int_V \nabla \times \boldsymbol{U}_M^* \cdot \nabla \times \boldsymbol{U}_N \,\mathrm{d}V. \end{aligned}\right\} \tag{64}$$

Using the analytical expression for QGIW modes given by (57)–(59), all the integrals in (64) can be explicitly evaluated. The surface integral is given by

$$\begin{aligned} \mathscr{G}_{MN} &= \int_S \boldsymbol{U}_M^* \cdot \boldsymbol{U}_N \,\mathrm{d}S \\ &= \sum_{i=0}^{N} \sum_{j=0}^{N-i} \sum_{k=0}^{M} \sum_{l=0}^{M-k} \pi 2^{j+l+m-1} \frac{C_{ijmN}}{Q_N} \frac{C_{klmM}}{Q_M} \sigma_N^{2i-1} \sigma_M^{2k-1} \left(1 - \sigma_N^2\right)^j \left(1 - \sigma_M^2\right)^l \\ &\quad \times \frac{(m + j + l - 1)!(2i + 2k - 3)!!}{[2(m + j + l + i + k) - 1]!!} \left\{ \frac{\sigma_N \sigma_M \hat{L}[2(i + k) - 1]}{\left(1 - \sigma_N^2\right)\left(1 - \sigma_M^2\right)} + 8ik(m + j + l) \right\}, \end{aligned} \tag{65}$$

where

$$\hat{L} = (2j\sigma_N + m\sigma_N + m)(2l\sigma_M + m\sigma_M + m) + (2j + m\sigma_N + m)(2l + m\sigma_M + m).$$

The volume integral in (64) is given by

$$\begin{aligned} \mathscr{F}_{MN} &= \int_V \nabla \times \boldsymbol{U}_M^* \cdot \nabla \times \boldsymbol{U}_N \,\mathrm{d}V \\ &= \sum_{i=0}^{N} \sum_{j=0}^{N-i} \sum_{k=0}^{M} \sum_{l=0}^{M-k} \pi 2^{j+l+m-1} \frac{C_{ijmN}}{Q_N} \frac{C_{klmM}}{Q_M} \sigma_N^{2i-1} \sigma_M^{2k-2} \left(1 - \sigma_N^2\right)^j \left(1 - \sigma_M^2\right)^l \\ &\quad \times \frac{(m + j + l - 1)!(2i + 2k - 3)!!}{[2(m + j + l + i + k) - 1]!!} \\ &\quad \times \left\{ \frac{\sigma_N \sigma_M \hat{L} 4ik[2(i + k) - 3]}{\left(1 - \sigma_N^2\right)\left(1 - \sigma_M^2\right)} + 8ik(2i - 1)(2k - 1)(m + j + l) \right\}. \end{aligned} \tag{66}$$

With the analytical expression $\boldsymbol{r} \cdot \boldsymbol{u}_0$ available, we can solve the heat equation (16) by expanding the temperature Θ_0 in terms of spherical harmonics $(P_l^m(\theta)\mathrm{e}^{\mathrm{i}m\phi})$ and

spherical Bessel functions $j_l(r)$, which leads to

$$\Theta_0 = \sum_{l,k,N} \frac{C_N P_l^m(\cos\theta) j_l(\xi_k r)}{4\pi j_{l+1}^2(\xi_{lk})\left(E\xi_{lk}^2 + i\sigma Pr\right)} \int_V \boldsymbol{U}_N \cdot \boldsymbol{r} P_l^m(\cos\theta) j_l(\xi_{lk} r)\,\mathrm{d}V \tag{67}$$

and

$$\int_V \boldsymbol{U}_M^* \cdot \boldsymbol{r}\Theta_0\,\mathrm{d}V = \sum_N C_N \mathscr{Z}_{MN}, \tag{68}$$

where

$$\mathscr{Z}_{MN} = \sum_{l,k} \frac{\left(E\xi_{lk}^2 - \mathrm{i}\sigma Pr\right)}{4\pi\left(E^2\xi_{lk}^4 + \sigma^2 Pr^2\right) j_{l+1}^2(\xi_{lk})} \left[\int_V \boldsymbol{U}_M^* \cdot \boldsymbol{r} P_l^m j_l(\xi_{lk} r)\,\mathrm{d}V \int_V \boldsymbol{U}_N \cdot \boldsymbol{r} P_l^m j_l(\xi_{lk} r)\,\mathrm{d}V\right]$$

with

$$\frac{1}{4\pi}\int_S \left[P_l^m(\cos\theta)\mathrm{e}^{\mathrm{i}m\phi}\right]\left[P_n^m(\cos\theta)\mathrm{e}^{\mathrm{i}m\phi}\right]^* \mathrm{d}S = \delta_{ln}.$$

The value of ξ_{lk} is chosen such that

$$j_l(\xi_{lk}) = 0, \quad 0 < \xi_{l1} < \xi_{l2} < \xi_{l3} < \cdots \quad \text{for} \quad l = m, m+2, m+4\cdots.$$

The problem for the onset of thermal convection then reduces to solutions of the algebraic equation

$$C_M \mathrm{i}(\sigma - \sigma_M) = E\sum_N \left(R_0 \mathscr{Z}_{MN} - \mathscr{F}_{MN} + 2\mathscr{G}_{MN}\right) C_N \quad \text{for} \quad M = 1, 2, 3, \ldots, \tag{69}$$

which is valid for $0 \leqslant Pr/E < \infty$ at $E \ll 1$. For given E, m, Pr and the half-frequencies σ_N of QGIW modes (such as those shown in table 1), (69) can be readily solved to determine the values of R_0, σ and the complex coefficients C_N, $N = 1, 2, 3\ldots$, for the onset of convection. The smallest Rayleigh number obtained, denoted by $(R_c)_{QGIW}$, represents the critical or most unstable mode of thermal convection in a rapidly rotating sphere.

4.4. *The limit* $Pr/E \to 0$

In the limit $Pr/E \to 0$, different QGIW modes in (69) are completely decoupled since the right-hand side of the equation becomes independent of σ. In consequence, the summation of the QGIW modes in (63) or on the right-hand side of (69) reduces to a single QGIW mode, $\boldsymbol{U}_K$, with its half-frequency σ_K. By replacing the summation $\sum_N$ with a single term and letting $\sigma = \sigma_M$, $M = N = K$ and $C_K = (1, 0)$, (69) becomes

$$0 = R_0 \mathscr{Z}_{KK} - \mathscr{F}_{KK} + 2\mathscr{G}_{KK}. \tag{70}$$

In other words, the half-frequency σ and the Rayleigh number R_0 at the onset of convection in the limit $Pr/E \to 0$ for a given azimuthal wavenumber m are

$$\sigma = \sigma_K, \tag{71}$$

$$R_0 = \frac{1}{\mathscr{Z}_{KK}}\left[-2\int_S \boldsymbol{U}_K^* \cdot \boldsymbol{U}_K\,\mathrm{d}S + \int_V \nabla \times \boldsymbol{U}_K^* \cdot \nabla \times \boldsymbol{U}_K\,\mathrm{d}V\right]. \tag{72}$$

The most unstable convection mode in a rapidly rotating sphere in the limit $Pr/E \to 0$ is found by calculating (72) for different wavenumbers m and K. When $m = 1$ and $K = 1$, we found that the Rayleigh number R_0 reaches its minimum, which yields

$$m_c = 1, \;\; R_c = 1.1254 \times 10^4 E, \;\; \sigma_c = \tfrac{1}{3}\left(1 + 2\sqrt{\tfrac{2}{5}}\right) \quad \text{for} \quad Pr/E \to 0. \tag{73}$$

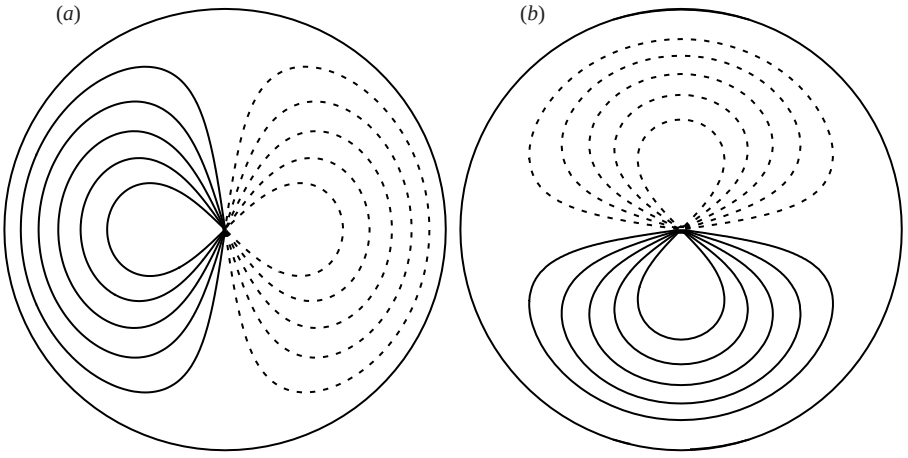

FIGURE 1. Contours of the radial velocity u_{0s} (a) and $u_{0\phi}$ (b) in the equatorial plane ($z=0$) for $m_c=1$ and $\sigma_c=0.7550$. Solid contours indicate $u_{0s}>0$ ($u_{0\phi}>0$) while dashed contours correspond to $u_{0s}<0$ ($u_{0\phi}<0$).

E	$(R_c)_{QGIW}$	$(\sigma_c)_{QGIW}$	$(R_c)_{FNUM}$	$(\sigma_c)_{FNUM}$
5×10^{-4}	5.627	0.7550	5.104	0.7550
5×10^{-5}	0.5627	0.7550	0.542	0.7550
5×10^{-6}	0.05627	0.7550	0.056	0.7550

TABLE 2. Comparison between the asymptotic and fully numerical results for the onset of convection in the limit $Pr/E\to0$ with $m_c=1$.

The corresponding analytical solution for the convective flow $\boldsymbol{u}_0$ can be written as

$$u_{0s}=\tfrac{15}{8}\left(1+\sqrt{\tfrac{2}{5}}\right)\left[1-s^2-\tfrac{5}{9}\left(\tfrac{13}{3}+4\sqrt{\tfrac{2}{5}}\right)z^2\right]\sin\left[\tfrac{2}{3}t\left(1+2\sqrt{\tfrac{2}{5}}\right)+\phi\right], \quad (74)$$

$$u_{0\phi}=\tfrac{15}{8}\left(1+\sqrt{\tfrac{2}{5}}\right)\left[1-\tfrac{5}{9}\left(5+\sqrt{\tfrac{2}{5}}\right)\left(1-\sqrt{\tfrac{2}{5}}\right)s^2-\tfrac{5}{9}\left(\tfrac{13}{5}+4\sqrt{\tfrac{2}{5}}\right)z^2\right]$$
$$\times\cos\left[\tfrac{2}{3}t\left(1+2\sqrt{\tfrac{2}{5}}\right)+\phi\right], \quad (75)$$

$$u_{0z}=\tfrac{15}{6}\left(1+2\sqrt{\tfrac{2}{5}}\right)sz\sin\left[\tfrac{2}{3}t\left(1+2\sqrt{\tfrac{2}{5}}\right)+\phi\right]. \quad (76)$$

Typical structure of the convective flow is shown in figure 1. It should be pointed out that, since there are no phase shifts in the radial direction of the flow, the differential rotation cannot be maintained by the Reynolds stresses of the convection in the form of a single inertial-wave mode given by (74)–(76).

We have also carried out the corresponding fully numerical simulations by solving (21)–(23) at $Pr=0$ for different values of E. Both the asymptotic and fully numerical results are shown table 2. A satisfactory agreement between the asymptotic relation given by (73) and the corresponding full numerics is achieved. Note that the values of $(R_c)_{QGIW}$ in table 2 for different values of E are calculated from the asymptotic relation (73).

Pr	$(R_c, m_c, \sigma_c)_{FNUM}$	$(R_c, m_c, \sigma_c)_{QGIW}$
0.023	(4.139, 1, −0.08722)	(4.161, 1, −0.08721)
0.10	(56.96, 1, −0.08390)	(56.96, 1, −0.08390)
0.25	(122.3, 5, −0.02833)	(122.6, 5, −0.02827)
0.70	(217.7, 7, −0.01956)	(216.9, 7, −0.01951)
1.00	(264.6, 8, −0.01633)	(263.5, 8, −0.01632)
7.00	(470.2, 12, −0.003177)	(468.6, 12, −0.003160)

TABLE 3. The critical Rayleigh numbers R_c, the preferred wavenumbers m_c and half-frequencies σ_c at the onset of convection for $E = 5 \times 10^{-5}$ with various Prandtl numbers.

4.5. *The general case* $0 < Pr/E < \infty$

We expect two primary effects when Pr increases from the limit $Pr/E \to 0$. First, more than one QGIW modes would be excited and sustained by thermal convection because the non-zero Pr in (69) couples a dominant QGIW mode with the neighbouring QGIW modes. Second, the interaction of different QGIW modes would result in the radial phase shift (spiralling) of the columnar convection roll and hence produce large Reynolds stresses (Zhang 1992).

Our discussion will focus on the two small Ekman numbers $E = 5 \times 10^{-5}$ and $E = 5 \times 10^{-6}$ for a wide range of the Prandtl number $0.023 \leqslant Pr \leqslant 7.0$, where $Pr = 0.023$ represents liquid gallium, which has been used in laboratory experiments (for example, Aurnou & Olson 2000; Aubert *et al.* 2001) and $Pr = 7.0$ is for water at room temperature. Our calculation to find critical value of the Rayleigh number R_c, the preferred azimuthal wavenumber m_c and the corresponding half-frequency σ_c for the onset of convection is systematic. For a given value of E and Pr, we have calculated all the relevant convection modes by solving (69) for various azimuthal wavenumbers in order to determine the critical mode that gives rise to the smallest Rayleigh number.

Table 3 shows two sets of the critical Rayleigh number R_c, the preferred wavenumber m_c and the corresponding half-frequency σ_c obtained at $E = 5 \times 10^{-5}$ for various values of Pr. One (with subscript $QGIW$) is obtained from the new method in a rotating sphere and the other (with subscript $FNUM$) is calculated from fully numerical simulations in a thick spherical shell with a small inner core $r_i/r_o = 0.01$. A satisfactory agreement between them is reached for all values of Pr.

The convection solutions obtained from the new method and the full numerics are very much alike in spatial structure, an example of which is displayed in figure 2 for $E = 5 \times 10^{-5}$ and $Pr = 0.25$ with $m_c = 5$. Some noticeable differences between the meridional plots are attributable to the different choices of meridional planes. It should be also pointed out that the new solution shown in figure 2(a) does not satisfy the stress-free boundary condition while the fully numerical solution satisfies all the required boundary conditions. However, the stress-free condition has been taken into account in the analysis for determining the critical parameters in connection with the vanishing surface integral in (64). An interesting question is which and how many QGIW modes are excited and sustained by convective instability. Table 4 displays the values of coefficients $|C_N|$ and the corresponding half-frequencies σ_N of the dominant QGIW modes. Note that the degree of polynomial for a QGIW mode $\boldsymbol{U}_N$ is $2N$. At $Pr = 0.023$, the convection is dominated by a single QGIW mode with $N = 1$, similar to that in the limit $Pr/E \to 0$. At $Pr = 0.25$, the chief dominant QGIW mode is shifted to $N = 3$ (with a polynomial of degree 6). Furthermore, the neighbouring modes with $N = 4, 2, 5$ also make significant contributions at $Pr = 0.25$. It is the coupling of

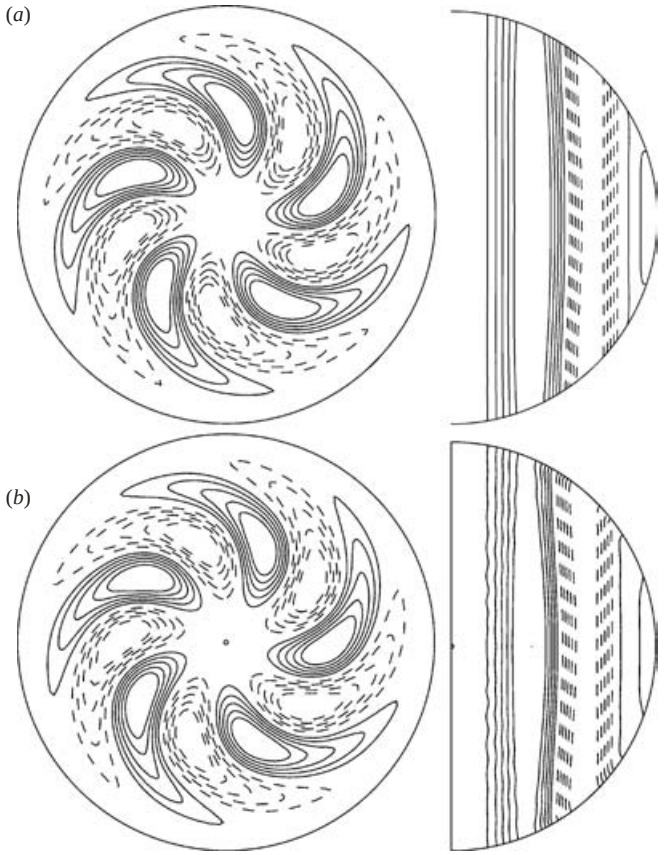

FIGURE 2. Contours of the radial velocity u_{0s} in the equatorial plane (left) and in a meridional plane (right) for $E = 5 \times 10^{-5}$ and $Pr = 0.25$. The solution in the full sphere based on the new method is shown in (*a*) while the corresponding fully numerical solution in a spherical shell with a small inner core is displayed in (*b*). Solid contours indicate $u_{0s} > 0$ and dashed contours correspond to $u_{0s} < 0$.

N	$\lvert C_N \rvert$	σ_N
3	1.0000	−0.04353
4	0.8652	−0.03030
2	0.5309	−0.06887
5	0.4756	−0.02241
6	0.1752	−0.01729

TABLE 4. Dominant coefficients $|C_N|$ and the corresponding half-frequencies σ_N derived from (69) for $E = 5 \times 10^{-5}$, $Pr = 0.25$ with the critical parameters at the onset of convection $(R_c)_{QGIW} = 122.6$, $(m_c)_{QGIW} = 5$, and $(\sigma_c)_{QGIW} = -0.02827$.

the neighbouring QGIW modes which is responsible for the spiralling structure of convection illustrated in figure 2.

When Pr increases further, both the critical wavenumber and the degree of the chief dominant QGIW mode increases accordingly. Figures 3 and 4 show the convection solutions obtained from the new method and full numerics at $E = 5 \times 10^{-5}$ for $Pr = 0.7$ and $Pr = 1.0$, respectively. Again both the solutions from the new method based on

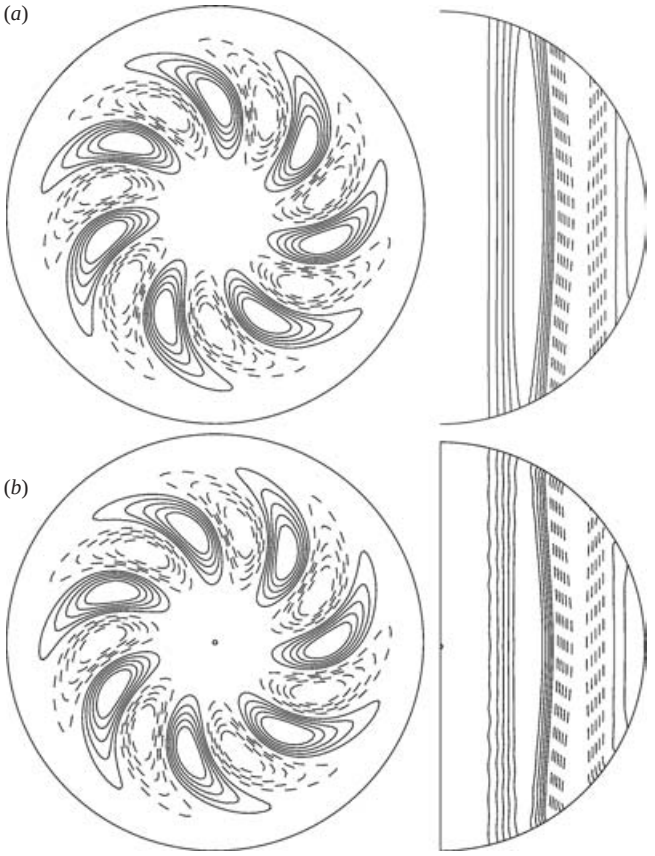

FIGURE 3. Contours of u_{0s} in the equatorial plane (left) and in a meridional plane (right) for $E = 5 \times 10^{-5}$ and $Pr = 0.7$ with $m_c = 7$. The solution in the full sphere based on the new method is shown in (*a*) while the corresponding fully numerical solution in a spherical shell with a small inner core is displayed in (*b*).

N	$\lvert C_N \rvert$	σ_N
4	1.0000	−0.03393
3	0.9884	−0.04731
5	0.6607	−0.02568
2	0.5041	−0.07194
6	0.3068	−0.02019
7	0.1078	−0.01632

TABLE 5. Dominant coefficients $|C_N|$ and the corresponding half-frequencies σ_N of QGIW modes derived from (69) for $E = 5 \times 10^{-5}$ and $Pr = 0.7$ with the critical parameters for the onset of convection $(R_c)_{QGIW} = 216.9$, $(m_c)_{QGIW} = 7$ and $(\sigma_c)_{QGIW} = -0.01951$.

QGIW modes and fully numerical simulations show very similar spatial structures. Tables 5 and 6 provide the values of coefficients $|C_N|$ and the corresponding half-frequencies σ_N of the dominant QGIW modes. For both the cases, the chief dominant QGIW mode is represented by a polynomial of degree 8.

At a smaller Ekman number $E = 5 \times 10^{-6}$, all the main characteristics of convection remain the same as those for $E = 5 \times 10^{-5}$. Table 7 shows the two sets of critical

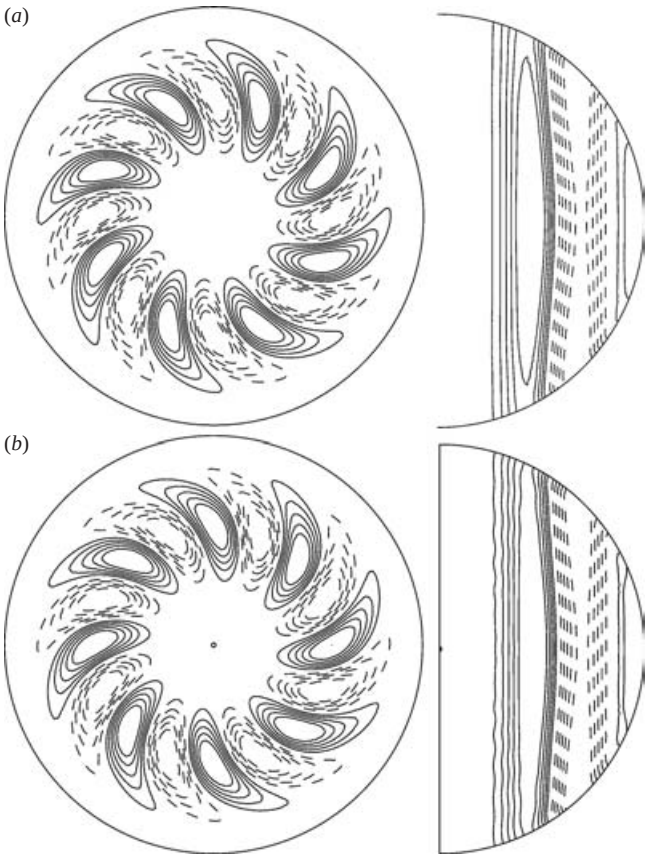

FIGURE 4. As figure 3 but for $Pr = 1.0$ with $m_c = 8$.

N	$\lvert C_N \rvert$	σ_N
4	1.00000	−0.035117
3	0.97756	−0.048407
5	0.66964	−0.026832
2	0.52343	−0.072509
6	0.32031	−0.021254
7	0.11696	−0.017295

TABLE 6. Dominant coefficients $|C_N|$ and the corresponding half-frequencies σ_N derived from (69) for $E = 5 \times 10^{-5}$ and $Pr = 1.0$ with the critical parameters at the onset of convection $(R_c)_{QGIW} = 263.5$, $(m_c)_{QGIW} = 8$ and $(\sigma_c)_{QGIW} = -0.01632$.

Rayleigh numbers, preferred wavenumbers and half-frequencies obtained at $E = 5 \times 10^{-6}$, showing again a satisfactory agreement between the results obtained from the new method and full numerics. For a sufficiently small Pr, for example, $Pr = 0.023$, the convection is dominated by a single equatorial-attached inertial mode (Zhang & Busse 1987; Zhang 1994) with $m_c = 8$ described by a quadratic polynomial of z and s. At a moderately small $Pr = 0.05$, a combination of several QGIW modes with the wavenumber $m_c = 8$ and polynomials of degrees 8, 10, 12 are excited and

Pr	$(R_c, m_c, \sigma_c)_{FNUM}$	$(R_c, m_c, \sigma_c)_{QGIW}$
0.023	(30.25, 8, −0.1246)	(30.10, 8, −0.1244)
0.05	(94.00, 8, −0.02823)	(93.37, 8, −0.02796)
0.10	(145.2, 11, −0.02110)	(146.0, 11, −0.02099)
0.70	(424.1, 16, −0.009528)	(427.0, 16, −0.009525)
1.00	(519.8, 17, −0.007778)	(515.1, 17, −0.007809)

TABLE 7. The critical Rayleigh numbers, the corresponding preferred wavenumbers and half-frequencies at the onset of convection at $E = 5 \times 10^{-6}$ for various Prandtl numbers. The full numerical solutions are obtained in a rotating spherical shell with a small inner sphere at $r_i/r_o = 0.01$.

N	$\lvert C_N \rvert$	σ_N
4	1.00000	−0.035117
5	0.79981	−0.026832
6	0.51072	−0.021254
3	0.36916	−0.048407
7	0.46908	−0.037259
9	0.22486	−0.017295
8	0.07667	−0.014371

TABLE 8. Dominant coefficients $|C_N|$ and the corresponding half-frequencies σ_N derived from (69) for $E = 5 \times 10^{-6}$ and $Pr = 0.05$ with the critical parameters at the onset of convection $(R_c)_{QGIW} = 93.37$, $(m_c)_{QGIW} = 8$ and $(\sigma_c)_{QGIW} = -0.02796$.

N	$\lvert C_N \rvert$	σ_N
6	1.00000	−0.023470
5	0.88285	−0.029094
7	0.80574	−0.001940
8	0.47288	−0.016334
4	0.46908	−0.037259
9	0.21276	−0.013964
10	0.08064	−0.012089

TABLE 9. Dominant coefficients C_N and the corresponding half-frequencies σ_N of the QGIW modes derived from (69) for $E = 5 \times 10^{-6}$ and $Pr = 0.1$ with the critical parameters for the onset of convection $(R_c)_{QGIW} = 146.0$, $(m_c)_{QGIW} = 11$ and $(\sigma_c)_{QGIW} = -0.02099$.

sustained by thermal instability, which is shown in table 8. When Pr increases to 0.1, the degree of the chief QGIW mode $\boldsymbol{U}_N$ increases to degree 12 (table 9) while the degree of the chief QGIW mode at $Pr = 1.0$ becomes 16. The structure of convection solutions obtained from the new method and full numerics are very similar and two examples are shown in figure 5 for $Pr = 0.05$ and $Pr = 0.1$. When the Ekman number is reduced further to $E = 10^{-6}$ for $Pr = 0.023$, we obtain a multi-humped convection mode which was first found by Ardes *et al.* (1997). In this case, the new method gives rise to $(R_c)_{QGIW} = 90.01$, $(m_c)_{QGIW} = 11$ and $(\sigma_c)_{QGIW} = -0.0254$ while the full numerics yields $(R_c)_{FNUM} = 91.98$,$(m_c)_{FNUM} = 11$ and$(\sigma_c)_{FNUM} = -0.0257$. In figure 6, we show the structure of both the equatorial-attached and multi-humped convection modes for $Pr = 0.023$ obtained from the new method and full numerics.

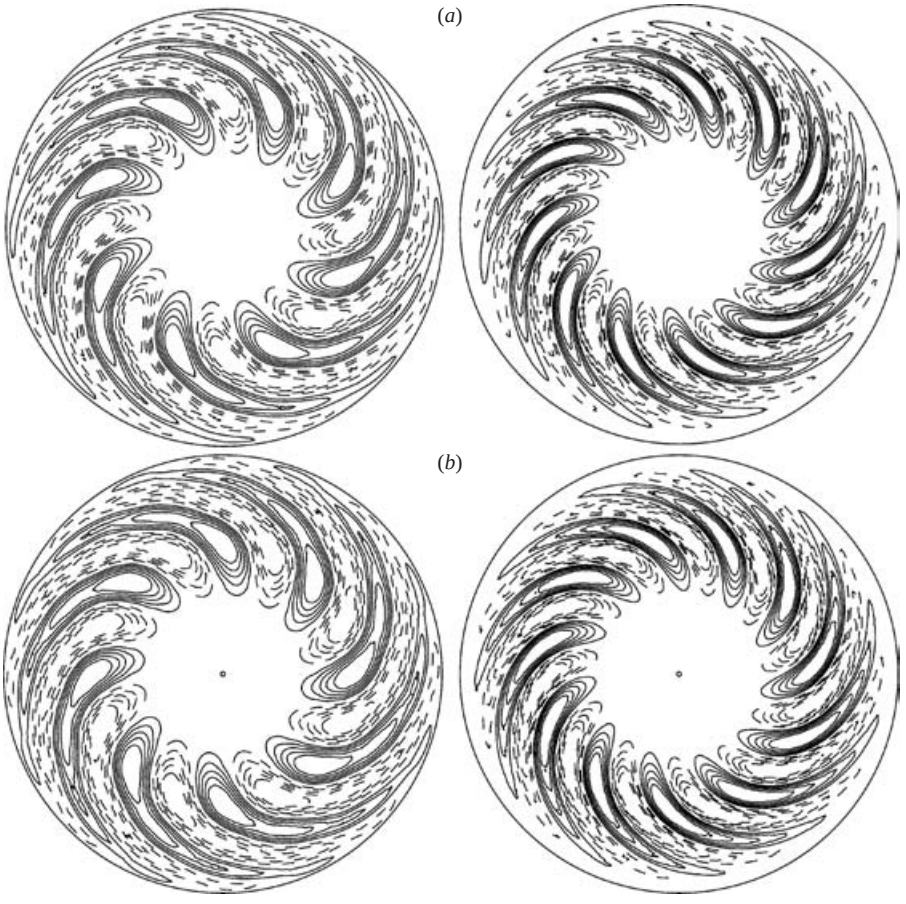

FIGURE 5. Contours of the radial velocity u_{0s} in the equatorial plane for $E = 5 \times 10^{-6}$. The solutions in the full sphere based on the new method are shown in (*a*) while the fully numerical solutions in a shell with a small inner core are displayed in (*b*). Left: for $Pr = 0.05$ with $m_c = 8$; right: $Pr = 0.1$ with $m_c = 11$.

In summary, we found a satisfactory agreement between the new method and full numerics for a wide range of the Prandtl number at $E \ll 1$. Our anticipation that the convective motion in a rapidly rotating sphere ($E \ll 1$) at the onset of convection, dependent upon the size of Pr/E, consists of either a single or several QGIW modes excited and sustained by thermal instabilities is confirmed.

4.6. *Differential rotation*

On the basis of a linear convection solution, we can determine both the amplitude and the profile of the convection-driven differential rotation $U(s)$ explicitly in terms of the dominant coefficients C_N given in previous tables such as table 9. We consider the ϕ-component of the momentum equation for the $O(\epsilon^2)$ problem in expansion (13):

$$\hat{\boldsymbol{\phi}} \cdot [\nabla \times (\boldsymbol{u}_0 + \boldsymbol{u}_0^*) \times (\boldsymbol{u}_0 + \boldsymbol{u}_0^*) + \nabla p_1] = \hat{\boldsymbol{\phi}} \cdot \nabla^2 (\hat{\boldsymbol{\phi}} U(s)), \tag{77}$$

where $\boldsymbol{u}_0$ is the linear solution at the onset of convection. Taking an azimuthal average of (77), we obtain

$$\hat{\boldsymbol{\phi}} \cdot [(\nabla \times \boldsymbol{u}_0 \times \boldsymbol{u}_0^*) + (\nabla \times \boldsymbol{u}_0^* \times \boldsymbol{u}_0)] = -\hat{\boldsymbol{\phi}} \cdot \nabla \times \nabla \times (\hat{\boldsymbol{\phi}} U(s)). \tag{78}$$

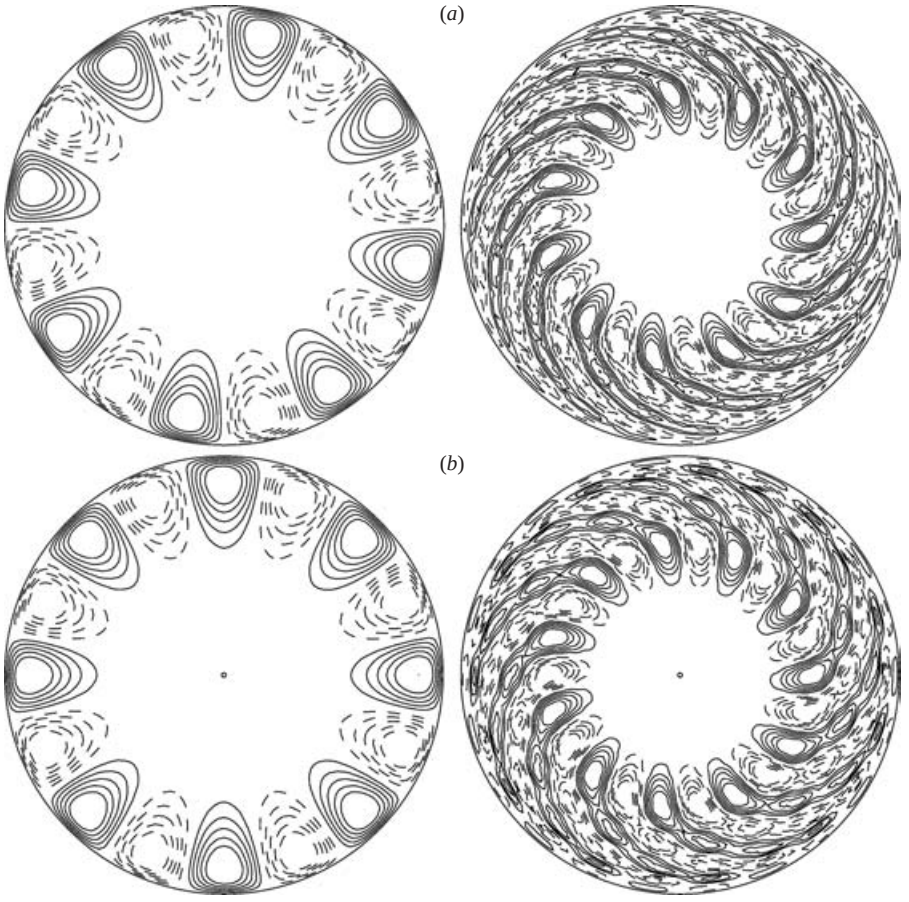

FIGURE 6. Contours of the radial velocity u_{0s} in the equatorial plane for $Pr = 0.023$. The solutions in the full sphere based on the new method are shown in (*a*) while the fully numerical solutions in a spherical shell with a small inner core are displayed in (*b*). Left: $E = 5 \times 10^{-6}$ with $m_c = 8$; right: $E = 10^{-6}$ with $m_c = 11$.

In deriving the differential rotation $U(s)$, it is more convenient to express a QGIW mode in cylindrical polar coordinates (s, ϕ, z)

$$\boldsymbol{U}_N = [\hat{\boldsymbol{s}} \cdot \boldsymbol{U}_N, \hat{\boldsymbol{\phi}} \cdot \boldsymbol{U}_N, \hat{\boldsymbol{z}} \cdot \boldsymbol{U}_N] = [\mathrm{i}U_{sN}, U_{\phi N}, \mathrm{i}U_{zN}]\mathrm{e}^{\mathrm{i}m\phi},$$

where the three real functions $(U_{Ns}, U_{N\phi}, U_{Nz})$, to leading approximation, can be written as

$$U_{zN} = z \sum_{j=0}^{N-1} \frac{C_{1jmN}}{Q_N} 2\sigma_N s^{m+2j} + O\left(\sigma_N^3\right), \tag{79}$$

$$U_{sN} = -\sum_{j=0}^{N} \frac{C_{0jmN}}{Q_N} (m + m\sigma_N + 2j\sigma_N) s^{m+2j-1} + O\left(\sigma_N^2\right), \tag{80}$$

$$U_{\phi N} = \sum_{j=0}^{N} \frac{C_{0jmN}}{Q_N} (m + m\sigma_N + 2j) s^{m+2j-1} + O\left(\sigma_N^2\right), \tag{81}$$

where $m = m_c \geqslant 1$. Making use of expansion (51), we can rewrite (78) in the form

$$\sum_{N,K} \mathrm{Im}[C_N C_K^* - C_N^* C_K] \frac{1}{\sigma_N} \frac{\partial U_{zN}}{\partial z} U_{sK} = -\hat{\boldsymbol{\phi}} \cdot \nabla \times \nabla \times (\hat{\boldsymbol{\phi}} U(s)). \tag{82}$$

By using the linear solution at the onset of convection, a second-order differential equation for $U(s)$ is derived:

$$\frac{\mathrm{d}}{\mathrm{d}s}\left[\frac{1}{s}\frac{\mathrm{d}}{\mathrm{d}s}(sU))\right] = \sum_{N,K} \frac{1}{Q_K Q_N} \mathrm{Im}[C_N C_K^* - C_N^* C_K]$$
$$\times \left[\sum_{j=0}^{N-1}\sum_{l=0}^{K} C_{1jmN} C_{0lmK} \left(1-\sigma_N^2\right)^j \left(1-\sigma_K^2\right)^{l-1} (2l\sigma_K + m\sigma_K + m) s^{2(j+l+m)-1}\right], \tag{83}$$

which can be readily solved together with the condition of the conservation of the total angular momentum in the fluid sphere

$$\int_0^1 \int_0^{\pi} U(r\sin\theta) r^3 \sin^2\theta \, \mathrm{d}r \, \mathrm{d}\theta = 0. \tag{84}$$

The solution of (83) yields an analytical expression for the mean flow produced by the nonlinear interaction of the convectively excited QGIW modes with a wavenumber m

$$U(s) = s \sum_{N,K} \frac{1}{Q_K Q_N} \mathrm{Im}\left[C_N C_K^* - C_N^* C_K\right] \sum_{j=0}^{N-1}\sum_{l=0}^{K} C_{1jmN} C_{0lmK} \left(1-\sigma_N^2\right)^j \left(1-\sigma_K^2\right)^{l-1}$$
$$\times \frac{(2l\sigma_K + m\sigma_K + m)}{4(j+l+m)(j+m+l+1)} \left[s^{2(j+l+m)} - \frac{2^{j+l+m} 15 (j+l+m+1)!}{[2(j+l+m)+5][2(j+l+m+3)]!!}\right]. \tag{85}$$

It follows that the differential rotation $U(s)$ can be explicitly computed by using the values of C_N and σ_N given in previous tables. This is the first explicit analytical expression for the convection-driven differential rotation in a rapidly rotating sphere.

There are two interesting features of the solution of the differential rotation driven by convection. First, it is geostrophic at the leading order, i.e. the flow profile is independent of the z-coordinate. More significantly, the amplitude of the mean flow, given by (ϵ^2/E), can be much larger than the amplitude of the convection ϵ when E is sufficiently small ($E \ll \epsilon$), which is in agreement with the existing numerical simulations. Two examples of the mean flow profile $U(s)$ are shown in figure 7 for $E = 5 \times 10^{-5}$ at $Pr = 1.0$ and for $E = 5 \times 10^{-6}$ at $Pr = 0.05$, which resemble those obtained from fully numerical simulations (e.g. Zhang 1992; Tilgner & Busse 1997, 1998). Both the linear solutions have the critical wavenumber $m_c = 8$ (see figures 4 and 5). The location of the maximum of $U(s)$ corresponds to the location of the convective rolls.

Greenspan (1969) demonstrated that there are no resonant nonlinear interactions of discrete inertial modes which can generate a strong differential rotation in a rotating inviscid fluid. His conclusion is not applicable to the present problem in which it is the nonlinear interaction of the convection modes defined by (51)–(53) that generates the differential rotation (85) in a rotating viscous fluid sphere. In other words, the

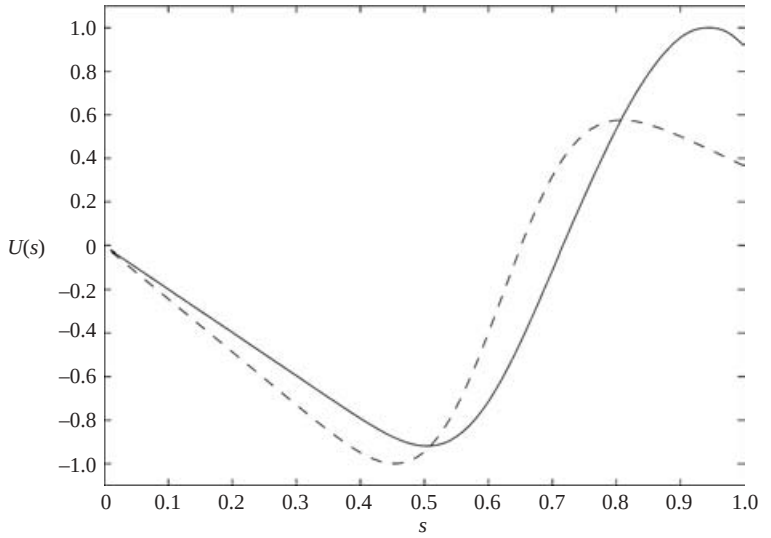

FIGURE 7. Normalized mean flows $U(s)$ as a function of s. Dashed line is for $E = 5 \times 10^{-5}$ and $Pr = 1.0$ and solid line is for $E = 5 \times 10^{-6}$ and $Pr = 0.05$. In both the cases, the most unstable modes of linear convection have the preferred wavenumber $m_c = 8$.

essential mechanism of the mean flow generation here is the same as that discussed by Busse (1976, 1983) and our governing equation (83) for the differential rotation is similar to equation (5.3*a*) in Busse (1983).

5. Concluding remarks

The subject of rotating fluid dynamics has been traditionally divided into two important but usually separate branches: the inertial-oscillation problem and the convective instability problem. The inertial problem describes the motion of an inviscid fluid in a rotating container, influenced weakly by viscous dissipation that mainly occurs near the walls in Ekman boundary layers. In the convection problem, internal viscous dissipation usually plays a key role in determining the basic properties of thermal convection in rotating fluids with an additional heat equation for the supply of energy. A classical treatment of the inertial problem in rotating fluids was given in Greenspan's (1968) monograph while a classical treatment of the convective problem in rotating fluids was given in Chandrasekhar's (1961) monograph.

An important contribution made by the analysis of this paper is to unite the two previously disjointed subjects in a rapidly rotating fluid sphere. We are able to demonstrate that the convective motion at very small Prandtl numbers $Pr/E \to 0$ is represented essentially by a single QGIW mode. In this case, the inertial wave carries the temperature and associated density differences passively and the buoyancy force maintains the convection against the weak viscous dissipation which primarily takes place in the Ekman boundary layers. The mean flow cannot be generated by the single QGIW mode. As the Prandtl number increases, more QGIW modes of higher degree are excited so that the viscous dissipation occurs in both the Ekman boundary layer and the interior. The nonlinear interaction of the convectively excited QGIW modes through the Reynolds stresses generates a strong zonal flow whose amplitude may be much larger than that of the most unstable non-axisymmetric convection.

r_i/r_o	$(R_c)_{FNUM}$	$(\sigma_c)_{FNUM}$
0.05	520.10	−0.007783
0.1	519.94	−0.007779
0.2	519.79	−0.007778
0.3	519.75	−0.007777
0.4	517.22	−0.007820
0.45	526.34	−0.008142
0.5	564.49	−0.008676

TABLE 10. The Rayleigh numbers and the corresponding half-frequencies at the onset of convection for $E = 5 \times 10^{-6}$ with various values of r_i/r_o for $m = 17$ and $Pr = 1.0$.

Theoretically speaking, the asymptotic theories for the highly localized convection (Roberts 1968; Busse 1970; Jones *et al.* 2000) would be valid for any value of Pr as long as $Pr/E \gg 1$ is satisfied. However, a satisfactory agreement between the asymptotic theories for the localized convection and full numerics has not been reached for $Pr \leqslant O(0.1)$, even at very small Ekman numbers $E \leqslant O(10^{-6})$. We believe that there are two possible explanations of why the agreement is poor for moderate values of Pr. The first is that $Pr/E = O(10^5)$ is still too small to be in the correct asymptotic regime for the theories. The second explanation may be that the nature of small-Pr convection, as shown in figure 6 for $Pr = 0.023$ (see also Simitev & Busse 2003), is characteristically different from that for $Pr \geqslant O(1)$.

Evidently, our new method can only be applicable to the convection problem in the whole sphere because an analytical expression for QGIW modes in a rotating spherical shell is not available. However, the presence of the inner core usually exerts insignificant influence on convection in rotating spherical shells when the size of the inner sphere is moderate (Busse & Cuong 1979; Dormy *et al.* 2004). To examine the effects of the inner sphere we can gradually increase $\eta = r_i/r_o$ while keeping all the other parameters unchanged. It is found that, for example at $E = 5 \times 10^{-6}$ with $Pr = 1.0$, the effect of the inner core on the main properties of convection is largely insignificant if $\eta < 0.45$, which is shown in table 10.

The type of the velocity boundary condition, whether it is stress free or non slip, does not enter the leading-order asymptotic theories for highly localized convection (Roberts 1968; Busse 1970; Soward 1977; Jones *et al.* 2000). The study in this paper is only concerned with convection in rapidly rotating spheres that have stress-free boundaries. It is the stress-free condition that enables us to derive a relatively simple algebraic equation (69) describing the onset of convection. While we expect weak influence of the velocity boundary condition on convection for moderate or large Prandtl numbers, the velocity boundary condition plays a critical role in determining the general properties of convection for small Prandtl numbers. However, it is not straightforward to extend the present method for the stress-free condition to that for rigid boundaries. This is because a general analytical expression for the spherical Ekman layers for all the QGIW modes is required and a matching between the Ekman boundary layers for all the QGIW modes and the interior convection solution must be be carried out. This important issue will be addressed in a future paper.

We are grateful to Professors F. H. Busse, C. A. Jones and P. H. Roberts for discussions on the problem. K. Z. is supported by UK PPARC and NERC grants while X. L. is supported by UK Royal Society and China NSF grants.

REFERENCES

Ardes, M., Busse, F. H. & Wicht J. 1997 Thermal convection in rotating spherical shells. *Phys. Earth Planet Inter.* **99**, 55–67.

Aubert, J., Brito, D., Nataf, H. C., Cardin, P. & Masson, J. P. 2001 A systematic experimental study of rapidly rotating spherical convection in water and liquid gallium. *Phys. Earth Planet Inter.* **128**, 51–74.

Aurnou, J. M. & Olson, P. L. 2000 Experiments on Rayleigh–Bénard convection, magnetoconvection and rotating magnetoconvection in liquid gallium. *J. Fluid Mech.* **430**, 283–307.

Aurnou, J. M. & Olson, P. L. 2001 Strong zonal winds from thermal convection in a rotating spherical shell. *Geophys. Res. Lett.* **28**, 2557–2560.

Busse, F. H. 1970 Thermal instabilities in rapidly rotating systems. *J. Fluid Mech.* **44**, 441–460.

Busse, F. H. 1976 A simple model of convection in Jovian atmosphere. *Icarus* **20**, 255–260.

Busse, F. H. 1983 A model of mean flows in the major planets. *Geophys. Astrophys. Fluid Dyn.* **23**, 152–174.

Busse, F. H. 1994 Convection driven zonal flows and vortices in the major planets. *CHAOS* **4**, 123–134.

Busse, F. H. 2002 Convective flows in rapidly rotating spheres and their dynamo action. *Phys. Fluids* **14**, 1301–1314.

Busse, F. H. & Cuong, P. G. 1979 Convection in rapidly rotating spherical fluid shells. *Geophys. Astrophys. Fluid Dyn.* **8**, 17–41.

Busse, F. H. & Simitev, R. 2004 Inertial convection in rotating fluid spheres. *J. Fluid Mech.* **498**, 23–30.

Carrigan, C. R. & Busse, F. H. 1983 An experimental and theoretical investigation of the onset of convection in rotating spherical shells. *J. Fluid Mech.* **126**, 287–305.

Chandrasekhar, S. 1961 *Hydrodynamic and Hydromagnetic Stability*. Clarendon.

Christensen, U. R. 2001 Zonal flow driven by deep convection in the major planets. *Geophys. Res. Lett.* **28**, 2553–2556.

Christensen, U. R. 2002 Zonal flow driven by strongly supercritical convection in rotating spherical shells. *J. Fluid Mech.* **470**, 115–133.

Dormy, A. M., Soward, A. M., Jones, C. A., Jault, D. & Cardin, P. 2004 The onset of thermal convection in rotating spherical shells. *J. Fluid Mech.* **501**, 43–70.

Fearn, D. R., Roberts, P. H. & Soward, A. M. 1988 Convection, stability and the dynamo. In *Energy, Stability and Convection* (ed. B. Straughan & P. Galdi), pp. 60–324. Longman.

Greenspan, H. P. 1968 *The Theory of Rotating fluids*. Cambridge University Press.

Greenspan, H. P. 1969 On the non-linear interaction of inertial modes. *J. Fluid Mech.* **36**, 257–264.

Grote, E. & Busse, F. H. 2001 Dynamics of convection and dynamos in rotating spherical fluid shells. *Fluid Dyn. Res.* **28**, 349–368.

Grote, E., Busse, F. H. & Tilgner, A. 2000 Regular and chaotic spherical dynamos. *Phys. Earth Plant. Inter.* **117**, 259–272.

Gubbins, D. & Roberts, P. H. 1987 Magnetohydrodynamics of the Earth's core. In *Geomagnetism*, Vol. 2 (ed. J. A. Jacobs), pp. 1–183. Academic.

Jones, C. A., Mussa, A. I. & Worland, S. J. 2002 Magnetoconvection in a rapidly rotating sphere: the weak-field case. *Proc. R. Soc. Lond.* A **459**, 773–797.

Jones, C. A., Soward, A. M. & Mussa, A. I. 2000 The onset of thermal convection in a rapidly rotating sphere. *J. Fluid Mech.* **405**, 157–179.

Liao, X., Zhang, K. & Earnshaw, P. 2001 On the viscous damping of inertial oscillation in planetary fluid interiors. *Phys. Earth Planet. Inter.* **128**, 125–136.

Olson, P. L. & Glatzmaier, G. A. 1995 Magnetoconvection in a rotating spherical shell: structure of flow in the outer core. *Phys. Earth Planet. Inter* **92**, 109–118.

Roberts, P. H. 1968 On the thermal instability of a self-gravitating fluid sphere containing heat sources. *Phil. Trans. R. Soc. Lond.* A **263**, 93–117.

Sarson, G. R., Jones, C. A. & Longbottom, A. W. 1998 Convection driven geodynamo models of varying Ekman number. *Geophys. Astrophys. Fluid Dyn.* **88**, 225–259.

Simitev, R. & Busse, F. H. 2004 Patterns of convection in rotating spherical shells. *New J. Physics* **5**, 97.1–97.20.

Soward, A. M. 1977 On the finite amplitude thermal instability of a rapidly rotating fluid sphere. *Geophys. Astrophys. Fluid Dyn.* **9**, 19–74.

Soward, A. M. & Jones, C. A. 1983 The linear stability of the flow in the narrow gap between two concentric rotating spheres. *Q. J. Mech. Appl. Maths* **26**, 19–42.

Sumita, I. & Olson, P. L. 2000 Laboratory experiments on high Rayleigh number thermal convection in a rapidly rotating hemispherical shell. *Phys. Earth Planet. Inter.* **117**, 153–170.

Tilgner, A. & Busse, F. H. 1997 Finite amplitude convection in rotating spherical fluid shells. *J. Fluid Mech.* **332**, 359–376.

Tilgner, A. & Busse, F. H. 1998 Differential rotation generated by convection in rotating spheres. *Z. Angew. Math. Mech.* **78**, S765–S766.

Zhang, K. 1992 Spiralling columnar convection in rapidly rotating spherical fluid shells. *J. Fluid Mech.* **236**, 535–556.

Zhang, K. 1994 On coupling between the Poincaré equation and the heat equation. *J. Fluid Mech.* **268**, 211–229.

Zhang, K. & Busse, F. H. 1987 On the onset of convection in rotating spherical shells. *Geophys. Astrophys. Fluid Dyn.* **39**, 119–147.

Zhang, K., Earnshaw, P., Liao, X. & Busse, F. H. 2001 On inertial waves in a rotating fluid sphere. *J. Fluid Mech.* **437**, 103–119.

Zhang, K., Liao, X. & Earnshaw, P. 2004 On inertial waves and oscillations in a rapidly rotating fluid spheroid. *J. Fluid Mech.* **504**, 1–40.